JMEPEG
DOI: 10.1007/s11665-014-1071-z

1059-9495/$19.00

Optimization of Shape-Memory Effect in Fe-Mn-Si-Cr-Re Shape-Memory Alloys

Kun-Ming Lin, Jian-Hung Chen, Chen-Chih Lin, Cheng-Hsien Liu, and Hsin-Chih Lin

(Submitted September 15, 2013; in revised form April 30, 2014)

Fe-Mn-Si-Cr-based shape-memory alloys have excellent properties of formability, shape-memory effect, and low cost. These properties make Fe-Mn-Si-Cr SMAs ideal candidates for the application of pipe coupling and fish plates. In this study, we add slight Rhenium (Re, 0.05-0.3 wt.%) to Fe-30Mn-6Si-5Cr alloys to improve their shape-memory effect. The martensitic transformation, crystal structure, and aging precipitate of the Fe-30Mn-6Si-5Cr-Re alloys are analyzed. The optimization of shape-memory performance of Fe-30Mn-6Si-5Cr-Re alloys can be achieved efficiently by the proper combined treatments of pre-strain, aging, and shape-memory training.

Keywords aging, Fe-Mn-Si-Cr based shape-memory alloy, rhenium, shape-memory training

1. Introduction

Fe-Mn-Si-Cr-based shape-memory alloys (SMAs) have desirable formability, shape-memory effect (SME), and lower cost compared to Ti-Ni SMAs. These properties make Fe-Mn-Si-Cr SMAs ideal candidates for the application of pipe coupling and fish plates (Ref 1). In the past decades, extensive studies of the Fe-Mn-Si and Fe-Mn-Si-Cr SMAs were made focusing on the transformation behaviors (Ref 2-4), physical properties (Ref 3-5), effects of thermo-mechanical training (Ref 6-9), and composition dependence of SME and corrosion resistance (Ref 10-15). Hsu and co-authors (Ref 16, 17) reported that slight addition of rare earth (R.E.) element could improve the shape-memory performance of Fe-Mn-Si and Fe-Mn-Si-Cr alloys. The authors suggested that the slight addition of R.E. into these alloys might reduce the stacking fault energy, enhance the formation of thermal or stress-induced martensite, lower the T_N temperature, strengthen the austenite, and refine the grain size. These possible effects were considered to improve the shape-memory performance of Fe-Mn-Si and Fe-Mn-Si-Cr alloys. However, the R.E. always comprises many coexisting elements, such as La, Ce, Pr, etc. These coexisting elements might have their individual contribution on the alloy's properties, but their quantities could not be easily and precisely controlled. In a previous study (Ref 18), high purity of Rhenium (Re, atomic number: 75) was used to replace the R.E. elements to improve the SME of Fe-Mn-Si-Cr alloys. By precise addition of a single element, instead of comprising many uncertain elements, the exact effects of Re-addition can be clearly illuminated, which should be more beneficial for the real applications of Fe-Mn-Si-Cr alloys. In this study, by slight Re-addition (0.05, 0.1, 0.3 wt.%) into a Fe-30Mn-6Si-5Cr shape-memory alloy, we continue to investigate the crystal structure, shape-memory performance, aging precipitate, and shape-memory training of the Fe-30Mn-6Si-5Cr-Re alloys. Meanwhile, the combined treatments are provided for the Fe-30Mn-6Si-5Cr-Re alloys to achieve their SME optimization.

2. Experimental

A vacuum melting technique was employed to prepare the Fe-30Mn-6Si-5Cr, Fe-30Mn-6Si-5Cr-0.05Re, Fe-30Mn-6Si-5Cr-0.1Re, and Fe-30Mn-6Si-5Cr-0.3Re (wt.%) alloys. The as-cast ingots were homogenized at 1100 °C for 24 h and then hot-rolled into 2.5-mm-thickness plates. During the repetitious processes of multi-pass rolling and subsequent annealing in furnace, specimens were really hot-rolled in the temperature range of about 700-1000 °C. The as-rolled ingots were annealed at 1100 °C for 2 h and water quenched. Specimens for various tests were carefully cut from these as-annealed plates. Some as-annealed specimens were then aged at 500-800 °C for 2 h.

The Fe-30Mn-6Si-5Cr-Re alloys were analyzed by an ICP-AES (Induction Coupled Plasma Atomic Emission Spectrometry) apparatus. The measured chemical compositions, being presented in Table 1, are similar to those nominal ones. Originating from both the purity of raw materials and the element evaporation during the melting process, a slight composition variation is found in Table 1. However, the slight composition variation is in the acceptable range and does not have significantly effect on the alloy's properties. The XRD analysis was carried out at room temperature using a Philips PW1710 x-ray diffractometer with Cu Kα radiation, 30 kV tube voltage, and 20 mA current. The shape-memory performance

This article is an invited paper selected from presentations at the International Conference on Shape Memory and Superelastic Technologies 2013, held May 20–24, 2013, in Prague, Czech Republic, and has been expanded from the original presentation.

Kun-Ming Lin, Department of Materials Science and Engineering, Feng Chia University, Taipei, Taiwan; and **Jian-Hung Chen, Chen-Chih Lin, Cheng-Hsien Liu, and Hsin-Chih Lin**, Department of Materials Science and Engineering, National Taiwan University, Taichung, Taiwan. Contact e-mail: hclinntu@ntu.edu.tw.

Published online: 28 May 2014

was examined by a bending test with a surface strain of 3%. The testing system and calculation of shape recovery have been presented in the previous paper (Ref 19). The experiments of shape-memory training were carried out on a multi-functional MTS (Model: CY-6040A4, made in Taiwan) tester equipped with a heating furnace. During the shape-memory training, the specimens were treated by the repetition of a small amount of tensile deformation (ε = 3%) at room temperature, released the applied stress, and then followed by a recovery heating at 300-600 °C for 15 min. The data were automatically recorded in a digital computer, and the stress-strain curves were then calculated and drawn from the raw data. The shape recovery during the shape-memory training with various recovery heating temperatures was automatically calculated from the data of recovery strain at each cycle. TEM specimens were prepared by jet electro-polishing at −25 °C with an electrolyte consisting of 3% $HClO_4$ and 97% C_2H_5OH by volume. TEM observation was carried out by a JEOL-1200 EX microscope at an operating voltage of 120 kV.

3. Results and Discussion

Figure 1 shows the shape recovery ratio as a function of aging temperature for the Fe-30Mn-6Si-5Cr-Re alloys. For the alloys without Re-addition, with 0.05, and 0.1% Re-addition, the aging under each temperature will increase their recovery ratios, as shown in Fig. 1(a), (b), and (c) curves, respectively. Higher aging temperature results in more increment of recovery ratio, except for 800 °C. Therefore, 700 °C aging increases recovery ratio the most for all three alloys with different Re-addition. As for the Fe-30Mn-6Si-5Cr-0.3Re (Fig. 1d), 500 °C aging increases the most recovery ratio. The increment of recovery ratio is less for higher aging temperature than 500 °C. The 800 °C aged specimen even exhibits a lower recovery ratio than the as-quenched specimen. All these phenomena will be more discussed in next paragraphs.

Table 1 also presents the martensitic starting transformation temperatures (M_s), measured by differentiate scanning calorimetry (DSC), for the Fe-30Mn-6Si-5Cr-Re alloys. The M_s temperatures for all alloys are below ambient temperature (25 °C), which ensures no occurrence of thermal-induced martensitic transformation. Besides, the alloys with more Re-addition have higher M_s temperatures. Namely, the alloys' M_s are more near the ambient temperature. Thus, the stress-induced $\gamma \rightarrow \varepsilon$ transformation at ambient temperature is easier for specimens with more Re-addition, and their recovery ratios are higher during SME test. According to the TEM-EDS compositional analysis, much more Re content is detected in stacking fault (SF) region than in the γ phase. It is then reasonable to propose that Re will segregate in SF region and somehow lower the SF energy. This feature makes the perfect dislocations break easily into partial dislocations to form SF. Therefore, Re segregation will increase the SF probability. SF serves as the nucleation site for $\gamma \rightarrow \varepsilon$ transformation, and therefore Re-addition contributes to the better SME performance. Besides, two other effects of Re-addition are also proposed here, namely the strengthening effects of grain-refining and aging precipitation. As shown in Fig 2, the alloys with more Re-addition have smaller grain sizes. This strengthens the γ-parent phase, and therefore contributes to a better SME. Re-addition will also promote the nucleation and growth rate of the precipitation in γ-parent phase. Precipitates with proper sizes will strengthen the γ-parent phase, confining dislocation glide during deformation of the alloy. Thus, the stress-induced $\gamma \rightarrow \varepsilon$ transformation will dominantly account for the deformation during SME test, and hence increase the alloy's recovery ratio. However, both too much Re-addition and too high aging temperature result in over aging quickly. The precipitation under over-aging state will decrease the strengthening of γ-parent phase and thus reduce the recovery ratio during SME test. Regarding SME increment, the optimal temperature of 2 h aging is 700 °C for 0, 0.05, and 0.1% Re added Fe-30Mn-6Si-5Cr alloys. Higher aging temperature such as 800 °C causes over aging and reduces the SME.

It is worthy to confirm the crystal structure before SME test of Fe-30Mn-6Si-5Cr-Re alloys. Figure 3(a) and (b) shows the XRD analyses of 700 °C aged Fe-30Mn-6Si-5Cr-0.1Re alloys prepared by mechanical polishing and electro-chemical polishing, respectively. The XRD measurements were made on the surface of the specimens at ambient temperature. The spectrum in Fig. 3(a) indicates that the γ austenite is the major existing phase, while some ε martensite exists. However, DSC results show that the M_s temperature of the specimen is lower than ambient temperature. This indicates that the alloy should have no thermal-induced martensite at ambient temperature. Therefore, it is reasonably believed that the ε martensite was stress induced during the mechanical polishing of the specimen surface. The mechanical polish applied a stress on the specimen surface, generating stress-induced martensite (SIM) on the surface, which was then detected by XRD. Electro-chemical polish was reported to avoid the surface SIM artifact (Ref 22), and thus we also used electro-chemical polish to prepare the XRD specimen. The specimen was mechanical polished, and then aged at 700 °C for 2 h in a vacuumed furnace. The specimens were then soaked in electrolytic solution (hydrogen peroxide:hydrofluoric acid = 10:1, volumetric ratio) as anode and graphite as cathode. The specimen was then electro-chemical polished at a voltage of 15 V and at ambient temperature for 40 s. As shown in Fig. 3(b) for the electro-polished specimen, no ε martensite is found anymore. This

Table 1 The ICP-AES measured compositions and DSC measured transformation temperatures of Fe30Mn6Si5Cr-Re alloys

	Elements (wt.%) and transformation temperatures						
Alloys	**Fe**	**Mn**	**Si**	**Cr**	**Re**	**M_s, °C**	**A_s, °C**
Fe-30Mn-6Si-5Cr	Bal.	30.0	6.0	5.1	0	4.32	121.36
Fe-30Mn-6Si-5Cr-0.05Re	Bal.	30.7	6.1	4.9	0.04	6.51	118.97
Fe-30Mn-6Si-5Cr-0.1Re	Bal.	30.5	5.9	4.9	0.09	12.20	117.81
Fe-30Mn-6Si-5Cr-0.3Re	Bal.	31.0	6.2	4.8	0.28	17.53	117.32

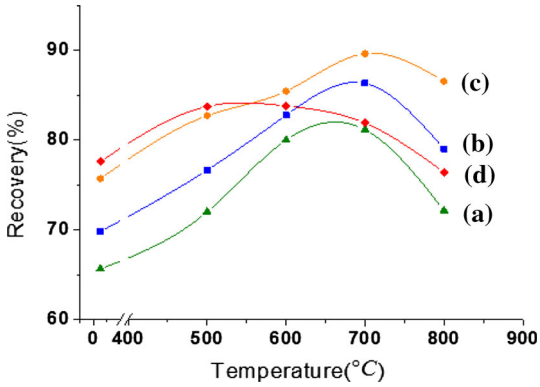

Fig. 1 The shape recovery ratio as a function of aging temperature for the Fe-30Mn-6Si-5Cr-Re alloys. (a) no Re-addition, (b) 0.05 Re, (c) 0.1 Re, (d) 0.3 Re

result proves that the ε martensite in Fig. 3(a) is a surface SIM artifact by mechanical polish.

It is interesting to analyze the aging precipitates of Fe-30Mn-6Si-5Cr-Re alloys. The aging precipitates could be observed in both the grain boundary and grain interior. Figure 4(a) and (b) shows the aging precipitates of Fe-30Mn-6Si-5Cr and Fe-30Mn-6Si-5Cr-0.1Re alloys, respectively. Both alloys were aged at 700 °C for 2 h. By analyzing the selected area diffraction pattern (SADP), the aging precipitates are identified as χ phase, which is of BCC structure. The lattice constant is about 0.89 nm. According to Yang et al. (Ref 20), the χ phase is an A12(α-Mn) prototype and has 58 atoms in a unit cell. The composition of χ phase is close to the matrix, but with apparently fewer Fe atoms and more of the other alloying elements. The TEM observation indicates that Re-addition promotes the nucleation and growth rate of the χ phase precipitation in γ-parent phase during aging of Fe-30Mn-6Si-5Cr-Re alloys.

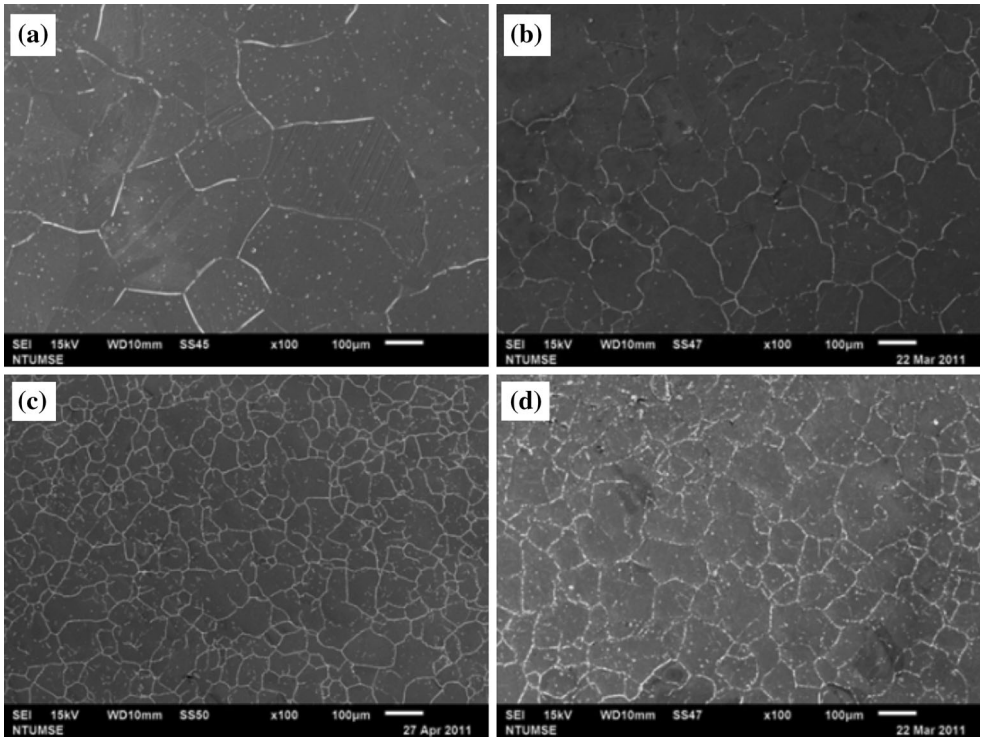

Fig. 2 The SEM secondary electron images of 700 °C × 2 h aged Fe-30Mn-6Si-5Cr-Re alloys. (a) no Re-addition, (b) 0.05 Re, (c) 0.1Re, (d) 0.3Re

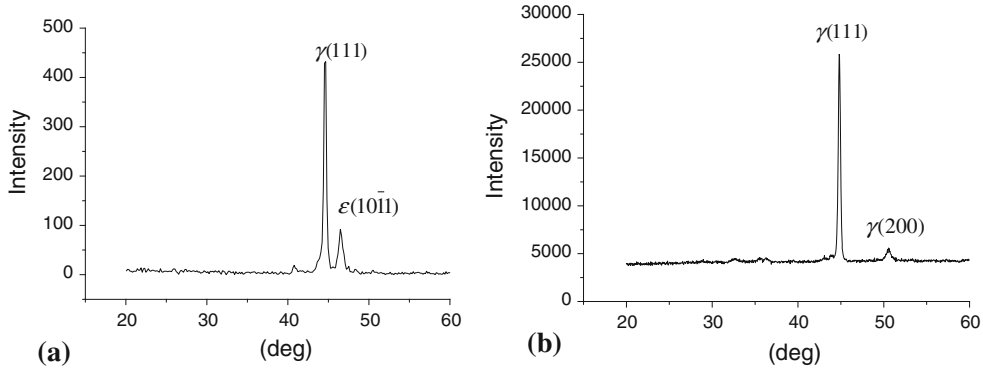

Fig. 3 XRD analyses of Fe-30Mn-6Si-5Cr-0.1Re prepared by (a) mechanical polish and (b) electro-chemical polish

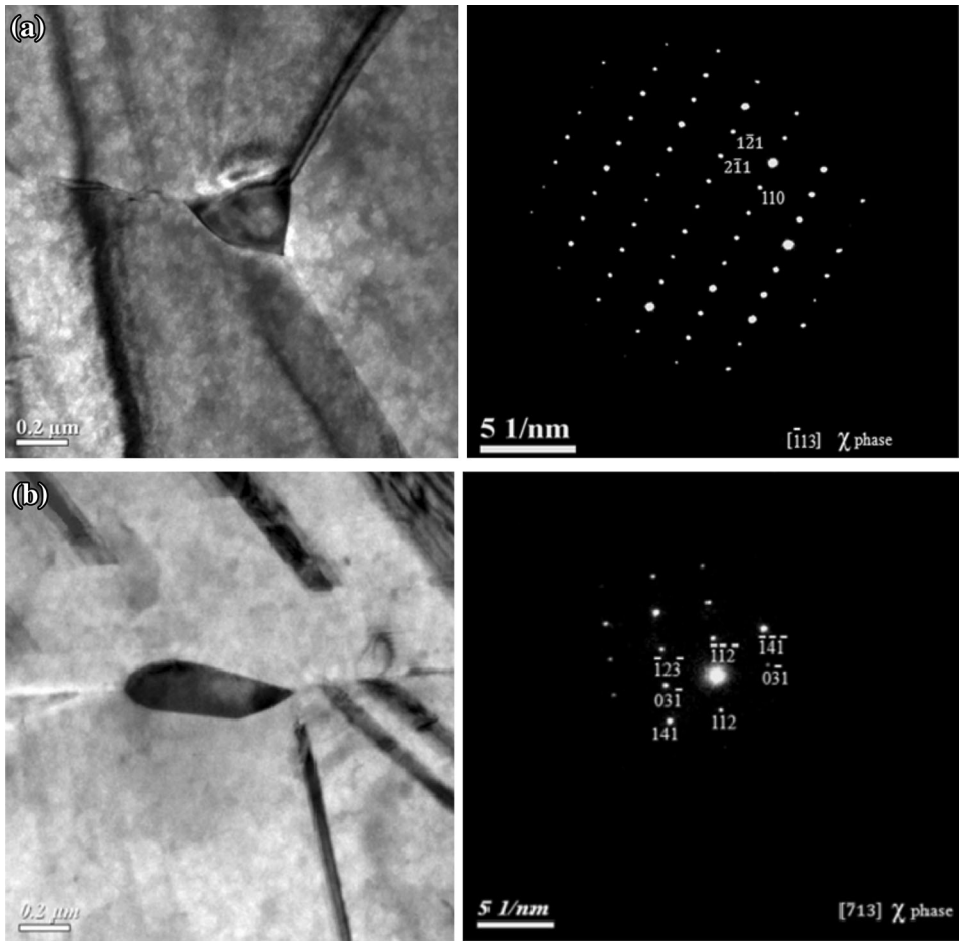

Fig. 4 TEM bright field images and SADPs of the χ phase in (a) Fe-30Mn-6Si-5Cr alloy and (b) Fe-30Mn-6Si-5Cr-0.1Re alloy. Both alloys were aged at 700 °C for 2 h

Figure 5 shows the shape recovery ratio as a function of training cycle for the Fe-30Mn-6Si-5Cr-0.1Re alloy, which has been subjected to shape-memory training with a 3% tensile strain and recovery heating at 300-600 °C for 15 min. As can be seen in Fig. 5, the shape recovery ratio increases with increasing training cycles at a recovery heating temperature of 500-600 °C, but decreases with increasing training cycles at a recovery heating temperature of 300 °C. This feature indicates that the stress-induced ε martensite by shape-memory training cannot be completely recovered to γ austenite at 300 °C. The residual ε martensite will hinder the formation of new ε martensite during the shape-memory test. Hence, the shape recovery ability is depressed because the plastic deformation during the shape-memory test is mainly contributed by the slip of perfect dislocations. Due to the accumulation of the irreversible ε martensite after cyclic training, the shape recovery ratio decreases with increasing training cycles, as shown in Fig. 5. However, at a higher recovery heating temperature of 500-600 °C, the shape recovery ratio increases with increasing training cycles. This comes from the fact that the stress-induced ε martensite by shape-memory training can be almost recovered to γ austenite and the new ε martensite during the shape-memory test can be easily induced by the applied stress. Besides, the retained effective nuclei of ε martensite can also promote the formation of new ε martensite. All these features will improve the specimen's shape-memory ability. Hence, the shape recovery ratio can significantly increase with increasing training cycles. The shape recovery ratio can even reach nearly 100% for the specimens with 6 training cycles and recovery heating at 500-600 °C.

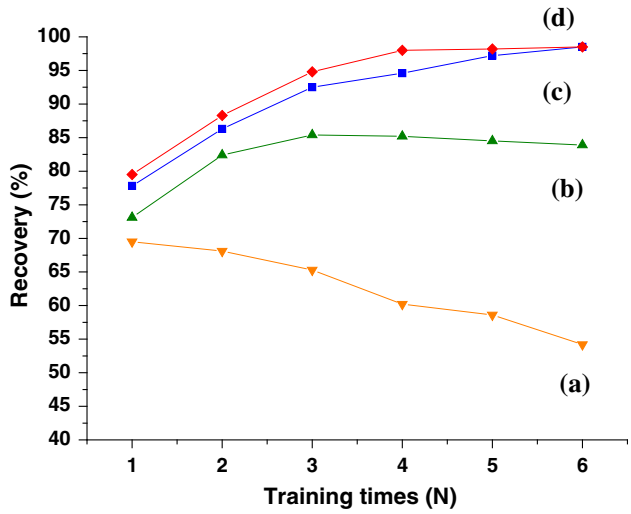

Fig. 5 Shape-memory training effect on SME for Fe-30Mn-6Si-5Cr-0.1Re specimens. The recovery heating temperatures are (a) 300 °C, (b) 400 °C, (c) 500 °C, and (d) 600 °C

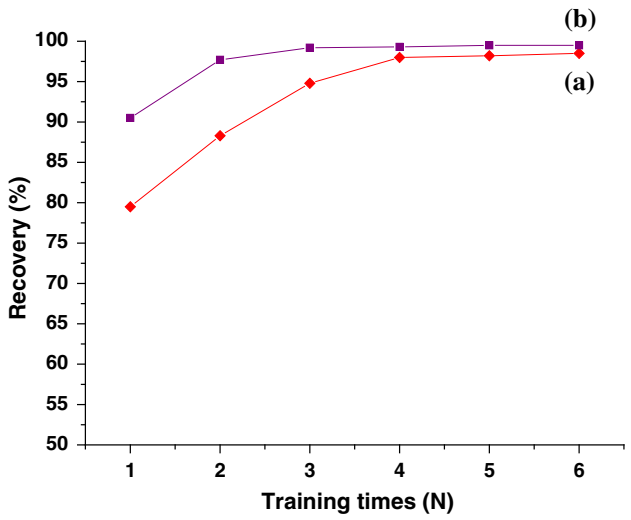

Fig. 6 Shape-memory training effect on SME for Fe-30Mn-6Si-5Cr-0.1Re specimens. (a) With aging at 700 °C for 2 h before training, (b) With 5% pre-stain, and aging at 700 °C for 2 h before training. The recovery heating temperature is 600 °C for the training

As discussed above, the shape memory of Fe-30Mn-6Si-5Cr-Re alloys can be improved effectively by suitable Re-addition, aging, and shape-memory training. Besides, the proper pre-strain before aging process is also expected to improve the alloy's shape-memory performance. It is reported (Ref 21) that the pre-strain introduces both defects and stress-induced martensite (SIM) in the alloy. The SIM recovers to austenite after aging, and the defects serve as nucleation sites of precipitation due to the residual stress around defects. The defects may promote the formation of aging precipitates within the grains and result in a better strengthening of γ phase after aging. Also, these defects may serve as nucleation sites of SIM, making the γ → ε transformation more easily. To optimize the SME performance, the specimens should be subjected to these combined treatments. In the present study, 5% pre-strain is carried out before the following aging treatment and shape-memory training process for the Fe-30Mn-6Si-5Cr-0.1Re alloy. In fact, we have carried out a series of pre-strain experiments for Fe-30Mn-6Si-5Cr-0.1Re alloys, including pre-strain of 0, 5, 10, and 15%. The 5% pre-strained specimen can exhibit the best shape-memory performance. Therefore, the pre-strain of 5% is carried out before the aging treatment and shape-memory training in this study. Figure 6 illustrates the effect of these combined treatments. The (b) curve presents the shape-memory training effect on the Fe-30Mn-6Si-5Cr-0.1Re which is 5% pre-stained and then 700 °C aged for 2 h before shape-memory training. The strain for shape-memory training is 3%, and the recovery heating temperature is 600 °C. Compared to the as-fabricated alloy ((a) curve), less training cycle is needed for nearly 100% recovery ratio. Therefore, the optimization of SME performance of Fe-30Mn-6Si-5Cr-Re alloy can be achieved efficiently by the proper combined treatments of pre-strain, aging, and shape-memory training.

4. Conclusions

Precipitation strengthening in the γ parent phase can effectively improve the SME recovery ratio in Fe-30Mn-6Si-5Cr alloys, except for the condition of over aging. Slight Re-addition promotes the precipitating of χ phase during aging of the alloys and increases the SME recovery ratio. Compared to as-quenched Fe-30Mn-6Si-5Cr alloy, 25% increment in recovery ratio is achieved by addition of 0.1 wt.% Re and 700 °C × 2 h aging. The shape-memory training, being deformed at room temperature and then heated to recovery temperature of 500 and 600 °C, could effectively improve the alloy's SME. This feature comes from the existence of nuclei for martensitic transformation after the shape-memory training. The optimization of SME performance of Fe-30Mn-6Si-5Cr-Re alloy can be achieved efficiently by the proper combined treatments of pre-strain, aging, and shape-memory training.

Acknowledgments

The authors are pleased to acknowledge the financial support of this research by the National Science Council (NSC), Republic of China, under Grant No. NSC 100-2221-E-002-101-MY3 and NSC 101-2221-E-035-020.

References

1. K. Yamauchi, et al., *Shape Memory and Superelastic Alloys*. Woodhead Publishing Limited, Boca Raton, 2011, p 141–159
2. A. Sato, E. Chishima, K. Soma, and T. Mori, Shape Memory Effect in γ ε Transformation in Fe-30Mn-1Si Alloy Single Crystals, *Acta Metall.*, 1982, **30**, p 1177–1183
3. H.C. Lin and K.M. Lin, An Investigation of Martensitic Transformation in an Fe-30Mn-6Si Shape Memory Alloys, *Scripta Metall. Mater.*, 1996, **34**, p 343–347
4. H.C. Lin, K.M. Lin, and T.S. Chou, A Study of Fe-30Mn-6Si Shape Memory Alloys Prepared from Different Melting Techniques, *Scripta Metall. Mater.*, 1996, **35**, p 879–884
5. A. Sato, Y. Yamaji, and T. Mori, Physical Properties Controlling Shape Memory Effect in Fe-Mn-Si Alloys, *Acta Metall.*, 1986, **34**, p 287–294
6. K. Tsuzaki, M. Ikegami, Y. Tomota, and T. Maki, Effect of Transformation Cycling on the ε Martensitic Transformation in Fe-Mn Alloys, *ISIJ*, 1990, **30**, p 666–673
7. B.H. Jiang, T. Tadaki, H. Mori, and T.Y. Hsu, In-situ TEM Observation of γ → ε Martensitic Transformation During Tensile Straining in an Fe-Mn-Si Shape Memory Alloy and In-situ TEM Observation of ε → γ Transformation During Heating in an Fe-Mn-Si Shape Memory Alloy, *Mater. Trans. JIM*, 1997, **38**(1072-1077), p 1078–1082
8. R.D. Xia, G.W. Liu, and T. Liu, The effect of thermal training on prestrained Fe-30Mn-6Si-5Cr shape memory alloy, *Mater. Lett.*, 1997, **32**, p 131–136
9. H.C. Lin, K.M. Lin, S.K. Wu, T.P. Wang, and Y.C. Hsia, Effects of Thermo-Mechanical Training on a $Fe_{59}Mn_{30}Si_6Cr_5$ Shape Memory Alloy, *Mater. Sci. Eng. A*, 2006, **438–440**, p 791–795
10. X.X. Wang and L.C. Zhao, The Effect of Thermal-Mechanical Training on the Formation of Stress-Induced ε Martensite in an Fe-Mn-Si-Ni-Co Alloy, *Scripta Metall. Mater.*, 1992, **26**, p 1451–1456
11. H.C. Lin, K.M. Lin, C.S. Lin, and T.M. Ouyang, The Corrosion Behavior of Fe-Based Shape Memory Alloys, *Corros. Sci.*, 2002, **44**, p 2013–2026
12. O. Soderberg, X.W. Liu, P.G. Yakovenko, K. Ullakko, and V.K. Lindroos, Corrosion Behaviour of Fe-Mn-Si Based Shape Memory Steels Trained by Cold Rolling, *Mater. Sci. Eng. A*, 1999, **273–275**, p 543–548
13. V.V. Bliznuk, V.G. Gavriljuk, B.D. Shanina, A.A. Konchits, and S.P. Kolesnik, Effect of Nitrogen and Carbon on Electron Exchange and Shape Memory in a Fe-Mn-Si Base Shape Memory Alloy, *Acta Mater.*, 2003, **51**, p 6095–6103
14. J.C. Li, W. Zheng, and Q. Jiang, Stacking Fault Energy of Iron-Base Shape Memory Alloys, *Mater. Lett.*, 1999, **38**, p 275–277
15. H. Kubo, K. Nakamura, S. Farjami, and T. Maruyama, Characterization of Fe-Mn-Si-Cr Shape Memory Alloys Containing VN Precipitates, *Mater. Sci. Eng. A*, 2004, **378**, p 343–348
16. W.M. Zhou, B.H. Jiang, X.A. Qi, and T.Y. Hsu, The Influence of Rare Earth Element on Shape Memory Effect in Fe-Mn-Si Alloys, *Scripta Metall. Mater.*, 1998, **39**, p 1483–1487

17. X. Huang, Y. Lei, B.L. Huang, S.P. Chen, and T.Y. Hsu, Effect of Rare-Earth Addition on the Shape Memory Behavior of a FeMnSiCr Alloy, *Mater. Lett.*, 2003, **57**, p 2787–2791
18. T.P. Wang, H.C. Lin, K.M. Lin, W.J. Wu, and P.C. Lo, Effects of Slight Re Addition on a Fe-25Mn-6Si-5Cr Shape Memory Alloy, *J. Comput. Theor. Nanosci.*, 2008, **5**, p 1753–1757
19. H.C. Lin and S.K. Wu, Strengthening Effect on Shape Recovery Characteristic of the Equiatomic TiNi Alloy, *Scripta Metall. Mater.*, 1992, **26**, p 59–62
20. C.H. Yang, H.C. Lin, K.M. Lin, and H.K. Tsai, Effects of Thermo-Mechanical Treatment on a Fe-30Mn-6Si Shape Memory Alloy, *Mater. Sci. Eng. A*, 2008, **497**, p 445–450
21. R.A. Shakoor and F.A. Khalid, Thermomechanical Behavior of Fe-Mn-Si-Cr-Ni Shape Memory Alloys Modified with Samarium, *Mater. Sci. Eng. A*, 2009, **499**, p 411–414
22. X.H. Min, T. Sawaguchi, K. Ogawa, T. Maruyama, F.X. Yin, and K. Tsuzaki, Shape memory effect in Fe-Mn-Ni-Si-C alloys with low Mn contents, *Mater. Sci. Eng. A*, 2011, **528**, p 5251–5258